Local inequalities for anisotropic finite elements and their application to convection-diffusion problems*

Thomas Apel† Gert Lube‡

March 30, 1995

Abstract. The paper gives an overview over local inequalities for anisotropic simplicial Lagrangian finite elements. The main original contributions are the estimates for higher derivatives of the interpolation error, the formulation of the assumptions on admissible anisotropic finite elements in terms of geometrical conditions in the three-dimensional case, and an anisotropic variant of the inverse inequality. An application of anisotropic meshes in the context of a stabilized Galerkin method for a convection-diffusion problem is given.

AMS(MOS) subject classification. 65N30, 65D05, 65N50

Key Words. anisotropic finite elements, interpolation error estimate, maximal angle condition, convection-diffusion problem, Galerkin/Least-squares

Contents

*The paper appeared as Preprint SPC94_26, TU Chemnitz-Zwickau.

†Technische Universität Chemnitz-Zwickau, Fakultät für Mathematik, D–09107 Chemnitz, Germany; email: na.apel@na-net.ornl.gov

‡Georg-August-Universtät Göttingen, Fachbereich Mathematik, Institut für Numerische und Angewandte Mathematik, Lotzestr. 16–18, D–37083 Göttingen, Germany; email: lube@namu01.gwdg.de

1 Introduction

If the solution of a partial differential equation has different behaviour in different space directions then it is an obvious idea to reflect this in a finite element approximation by using a family of meshes with different mesh sizes in different directions, so-called anisotropic meshes. Applications include the approximation of edge and interface singularities in diffusion dominated problems (Poisson type equations, Lamé system) [1, 3], of boundary and interior layers arising in convection-dominated problems [2, 10, 13, 15, 20, 21], of solutions of problems with strongly anisotropic material parameters, and of functions with different space and time behaviour [8].

However, the majority of papers in finite element theory and applications does not consider anisotropic elements, they are often explicitely excluded. As to the authors' knowledge, commercial finite element codes do not allow to use such elongated or flattened elements. Some reasons for this may be a lack in the classical finite element theory or the instance that anisotropic elements must be applied more carefully than isotropic ones for a good approximation. In this paper, we want to contribute to the theoretical foundation of anisotropic finite elements and to show an application of them.

For an introduction into the field we recall that the proof of finite element approximation properties is usually based on the knowledge of local interpolation error estimates. Here, we consider simplicial elements $e \subset \mathbb{R}^d$, $d = 2, 3$, and Lagrangian interpolation in spaces $\mathcal{P}_k$ of polynomials of maximal degree $k \geq 1$. The interpolant $I_h^{(k)} v$ of a continuous function v is uniquely determined by $(I_h^{(k)} v)(x^{(i)}) = v(x^{(i)})$, $i = 1, \ldots, n$, $n = \dim \mathcal{P}_k = \binom{k+d}{d}$, where $x^{(i)}$ are the nodal points of the element e.

In the classical interpolation theory, see for example [7], it is proved that for $v \in W^{k+1,p}(e)$, $p \in [1, \infty]$ and $m = 0, \ldots, k$, there holds

$$|v - I_h^{(k)} v; W^{m,p}(e)| \leq C \varrho_e^{-m} h_e^{k+1} |v; W^{k+1,p}(e)|, \tag{1.1}$$

where h_e and ϱ_e denote the diameters of the finite element e and of the largest inscribed ball in e, respectively, and $W^{k,p}(\,.\,)$ are the usual Sobolev spaces with the seminorm $|\,.\,; W^{k,p}(\,.\,)|$, see Section 2. Clearly, the assumption of a bounded aspect ratio,

$$h_e / \varrho_e \leq C_A, \tag{1.2}$$

which is equivalent to Zlámal's minimal angle condition, leads to the well-known estimate

$$|v - I_h^{(k)} v; W^{m,p}(e)| \leq C_I h_e^{k+1-m} |v; W^{k+1,p}(e)| \tag{1.3}$$

and the expectation that C_I would grow with C_A^m. Consequently, anisotropic elements with a very large ($h_e \gg \varrho_e$) or even unbounded ($h_e/\varrho_e \to \infty$ for $h_e \to 0$) aspect ratio were not considered for $m \geq 1$.

Yet in the mid-seventies the proof of (1.3) had been improved for some special cases of d, k, m, and p. The condition (1.2) was relaxed to a maximal angle condition (see Section 2) in [4] for $d = 2$, $k = 1, 2, 3$, $m = 1$, $p = 2$, and in [9] for $d = 2, 3$, $k = 1, 2, \ldots$, $m = 0, \ldots, k$, $p \in [1, \infty]$, $k + 1 - m > d/p$ for $p < \infty$, $k + 1 - m \geq 0$ for $p = \infty$. For some of these cases the assumptions were reformulated in [11, 12]. We remark that the case $d = 2$, $k = m = 1$, $p = \infty$ was already proved in 1957 [19]. Nevertheless these results were rarely applied because the possible advantage of using elements with different diameters in different directions was not exploited, only the largest of them is used in (1.3).

This remedy was removed in [1] by proving sharper (anisotropic) interpolation error estimates in the cases $d = 2, 3$, $m = 1$, and general k and p using a generalization of the Bramble-Hilbert theory [5, 6]. Here, the maximal angle condition and an additional coordinate system condition (see Section 2) are necessary. In [1], non-Lagrangian elements and rectangular elements were considered as well, and an application to edge singularities

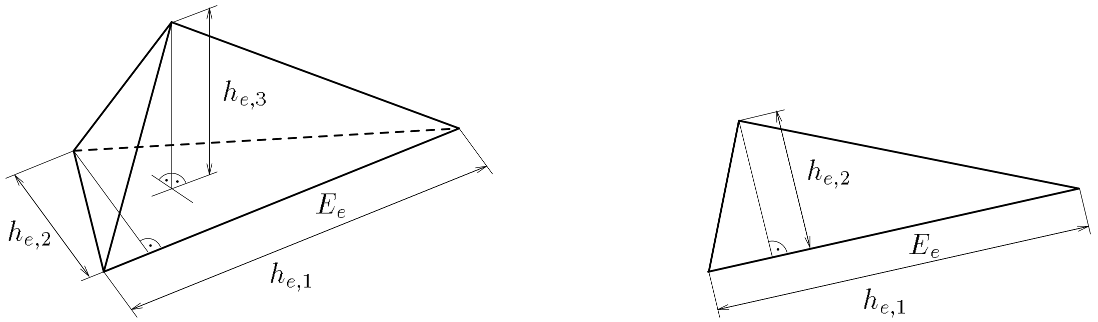

Figure 2.1: Illustration of the definition of the element related mesh sizes.

is given. We remark that the case $d = 2$, $m = 0$, $k = 1$, $p = 2$ was already treated in [16]. Anisotropic interpolation error estimates for functions from certain weighted Sobolev spaces were derived and applied in [3] ($d = 3$, $m = 1$, $k = 1$, $p > 2$). Moreover, anisotropic error estimates for meshes of tensor product type were used in the context of adaptive algorithms in [17, 18].

The outline of the paper is as follows: After the introduction of some notation we derive in Section 3 a slight extension of the classical inverse inequality which is useful in our application of anisotropic elements in stabilized Galerkin methods. In Section 4 we extend the local interpolation error estimates of [1] to general $m = 0, 1, \ldots, k$ (Theorem 4.2). A particular contribution is that we consider more detailed than in [1] the choice of the reference elements in three dimensions and the transformation to them (Appendix) which leads to an equivalent but more geometrical assumption on the admissible finite elements (maximal angle condition, coordinate system condition) than the more abstract setting in [1]. Moreover, we establish with Theorem 4.3 a weak anisotropic interpolation error estimate which holds also in the exceptional cases of Theorem 4.2. The results are summarized in Corollary 4.4 and allow also the statement of estimates in the form (1.3) for all these cases (Corollary 4.5). In Section 5, we prove the density of the family of finite element spaces in $W^{1,2}(\Omega)$ in the case of anisotropic meshes.

All these results are applied in the numerical analysis of stabilized Galerkin methods on general meshes in [2]. The main results of that paper are summarized in Section 6. Some numerical examples show the practical applicability of anisotropic meshes. In the last section we discuss the necessity of the maximal angle condition and the coordinate system condition.

2 Notation

To take advantage of the different sizes of the element e in different directions we introduce the following notation, compare Figure 2.1. For $e \subset I\!R^2$ let E_e be the longest edge of e. Then we denote by $h_{1,e} \equiv \mathrm{meas}_1(E_e)$ its length and by $h_{2,e} \equiv 2\,\mathrm{meas}_2(e)/h_{1,e}$ the diameter of e perpendicularly to E_e. In the three-dimensional case, we proceed by analogy. Let again E_e be the longest edge of e, and let F_e be the larger of the two faces of e with $E_e \subset \overline{F}_e$. Then we denote by $h_{1,e} \equiv \mathrm{meas}_1(E_e)$ the length of E_e, by $h_{2,e} \equiv 2\,\mathrm{meas}_2(F_e)/h_{1,e}$ the diameter of F_e perpendicularly to E_e, and by $h_{3,e} \equiv 6\,\mathrm{meas}_3(e)/(h_{1,e}h_{2,e})$ the diameter of e perpendicularly to F_e. Note that for the element sizes the relation $h_{1,e} \geq \ldots \geq h_{d,e}$ holds and that the element has the volume $\frac{1}{d!}h_{1,e}\cdots h_{d,e}$.

Introduce further an element related Cartesian coordinate system $(x_{1,e}, x_{2,e}, x_{3,e})$ such that $(0,0,0)$ is a vertex of $\hat{e}$, E_e is part of the $x_{1,e}$–axis, and F_e is part of the $x_{1,e}, x_{2,e}$–plane. For deriving interpolation error estimates we have to assume that the elements fulfill a maximal angle condition, see also [1, 4, 9, 11, 12] for equivalent formulations.

Maximal angle condition (2D): There is a constant $\gamma_* < \pi$ (independent of h and $e \in \mathcal{T}_h$) such that the maximal interior angle γ_e of any element e is bounded by $\gamma_* :\ \gamma_e \leq \gamma_*$.

Maximal angle condition (3D): There is a constant $\gamma_* < \pi$ (independent of h and $e \in \mathcal{T}_h$) such that the maximal interior angle $\gamma_{F,e}$ of the four faces as well as the maximal angle $\gamma_{E,e}$ between two faces of any element e is bounded by γ_* : $\gamma_{F,e} \le \gamma_*$, $\gamma_{E,e} \le \gamma_*$.

For anisotropic estimates we need additionally a coordinate system condition.

Coordinate system condition (2D): The element related coordinate system $(x_{1,e}, x_{2,e})$ can be transformed into the discretization independent coordinate system (x_1, x_2) via a translation and a rotation by an angle ψ_e, where $|\sin\psi_e| \le C h_{2,e}/h_{1,e}$.

Coordinate system condition (3D): The transformation of the element related coordinate system $(x_{1,e}, x_{2,e}, x_{3,e})$ into the discretization independent system (x_1, x_2, x_3) can be determined as a translation and three rotations around the $x_{j,e}$-axes by angles $\psi_{j,e}$ $(j = 1, 2, 3)$, where

$$|\sin\psi_{1,e}| \le C h_3/h_2, \quad |\sin\psi_{2,e}| \le C h_3/h_1, \quad |\sin\psi_{3,e}| \le C h_2/h_1. \tag{2.1}$$

Finally, let $W^{m,p}(e)$ $(m \in I\!N, p \in [1,\infty])$ be the usual Sobolev spaces with the norm and the special seminorm

$$\|v; W^{m,p}(e)\| \equiv \left\{ \sum_{|\alpha|\le m} \int_e |D^\alpha v|^p dx \right\}^{1/p}, \qquad |v; W^{m,p}(e)| \equiv \left\{ \sum_{|\alpha|= m} \int_e |D^\alpha v|^p dx \right\}^{1/p},$$

and the usual modification for $p = \infty$. We use a multi-index notation with

$$\alpha = (\alpha_1, \ldots, \alpha_d), \quad |\alpha| = \alpha_1 + \ldots + \alpha_d, \quad D^\alpha = \frac{\partial^{\alpha_1}}{\partial x_1^{\alpha_1}} \cdots \frac{\partial^{\alpha_d}}{\partial x_d^{\alpha_d}}, \quad h_e^\alpha = h_{1,e}^{\alpha_1} \cdots h_{d,e}^{\alpha_d}$$

the numbers α_i $(i = 1, \ldots, d)$ are non-negative integers.

Note that we use the symbol C for a generic positive constant, that means, C may be of different value at each occurrence. But C is always independent of the function under consideration, of the finite element mesh, and in Section 6 particularly of ε. On the contrary, some constants are indexed with a letter for later reference to them.

3 Inverse inequalities

We start with a lemma which the desired estimate can be derived from.

Lemma 3.1 *For $v \in \mathcal{P}_k(e)$, $k \in I\!N$ arbitrary, and $p \in [1,\infty]$, the estimate*

$$\left\| \frac{\partial v}{\partial x_i}; L^p(e) \right\| \le C h_{i,e}^{-1} \|v; L^p(e)\|, \quad i = 1, \ldots, d, \tag{3.1}$$

holds if and only if the coordinate system condition is satisfied for the element e.

Proof The transformation $x_{i,e} = h_{i,e}\tilde{x}_{i,e}$ $(i = 1, \ldots, d)$ transforms e to an element $\tilde{e}$ of which the largest inner ball has a diameter of order one. Thus we get from Theorem 3.2.6. of [7] (isotropic inverse inequality)

$$\left\| \frac{\partial \tilde{v}}{\partial \tilde{x}_{i,e}}; L^p(\tilde{e}) \right\| \le |\tilde{v}; W^{1,p}(\tilde{e})| \le C \|\tilde{v}; L^p(\tilde{e})\|, \quad i = 1, \ldots, d,$$

and after transforming back

$$\left\| \frac{\partial v}{\partial x_{i,e}}; L_p(e) \right\| \le C h_{i,e}^{-1} \|v; L^p(e)\|, \quad i = 1, \ldots, d. \tag{3.2}$$

Assume that the coordinate system condition is satisfied, and consider the two-dimensional case. Then we have with (3.2)

$$\begin{aligned}
\left\|\frac{\partial v}{\partial x_1}; L^p(e)\right\| &\leq |\cos\psi_e| \left\|\frac{\partial v}{\partial x_{1,e}}; L^p(e)\right\| + |\sin\psi_e| \left\|\frac{\partial v}{\partial x_{2,e}}; L^p(e)\right\| \\
&\leq C\left(h_{1,e}^{-1} + C\frac{h_{2,e}}{h_{1,e}} h_{2,e}^{-1}\right)\|v; L^p(e)\| \\
&= C h_{1,e}^{-1}\|v; L^p(e)\|.
\end{aligned}$$

The derivative $\frac{\partial v}{\partial x_2}$ and the three-dimensional case can be treated by analogy.

The necessity of the coordinate system condition is shown by an example. Consider the triangle with the vertices $(0,0)$, $(h_1,0)$, $(0,h_2)$ in the element related coordinate system $(x_{1,e}, x_{2,e})$ and the function $v = x_{2,e}$. Then we have

$$\begin{aligned}
\|v; L^p(e)\|^p &= \int_e x_{2,e}^p \, dx_e = \tfrac{1}{(p+1)(p+2)} h_{1,e} h_{2,e}^{p+1} \\
\left\|\frac{\partial v}{\partial x_1}; L^p(e)\right\|^p &= \int_e \left|\cos\psi_e \frac{\partial v}{\partial x_{1,e}} - \sin\psi_e \frac{\partial v}{\partial x_{2,e}}\right|^p dx_e = |\sin\psi_e|^p h_{1,e} h_{2,e}.
\end{aligned}$$

Hence, (3.1) implies $|\sin\psi_e| \leq C h_{2,e}/h_{1,e}$. □

Corollary 3.2 *Assume that for the element e the coordinate system condition holds. Then for $v \in \mathcal{P}_k$, $k \in I\!N$ arbitrary, the estimate*

$$\|\Delta v; L^p(e)\| \leq C\left(\sum_{i=1}^d h_{i,e}^{-p}\left\|\frac{\partial v}{\partial x_i}; L^p(e)\right\|^p\right)^{1/p} \tag{3.3}$$

holds for any $p \in [1,\infty]$.

Proof Use Lemma 3.1 for $w = \frac{\partial v}{\partial x_i}$, $i = 1, \ldots, d$. □

Note that the particular result

$$\|\Delta v; L^p(e)\| \leq C_s h_{d,e}^{-1} |v; W^{1,p}(e)| \tag{3.4}$$

can be proved without the coordinate system condition because the Laplace operator is independent of a rotation of the coordinate system, and the change in the seminorm (which appears for $p \neq 2$) during a rotation is bounded by a positive factor which depends only on d and p.

4 Local interpolation error estimates

For the proof of error estimates of the form

$$\|D^\gamma(v - I_h^{(k)} v), L^p(e)\| \leq C \sum_\alpha \sum_{|\beta|=|\gamma|} h^\alpha \|D^{\alpha+\beta} v, L^p(e)\|$$

we proceed in the usual way: (1) transformation of the left-hand side to some reference element $\hat{e}$, (2) estimation of the error on the reference element $\hat{e}$, (3) transformation of the right-hand side to the element e. We recall that the transformation can be realized by

$$x = F(y) = By + b \tag{4.1}$$

with $B \in I\!R^{d\times d}$, $b \in I\!R^d$, $d = 2,3$, $e = F(\hat{e})$, and that this is done to get estimates with powers of h and a constant which is independent of the actual element. Hence, we can also use a finite number of reference elements. The choice of appropriate elements $\hat{e}$ is discussed in Appendix A. Each reference element has the property that for each axis of the coordinate system $(y_1, \ldots, y_d)$ there is one edge of $\hat{e} \subset I\!R^d$ that has length one and is parallel to this axis. We will use this in the proof of Theorem 4.1 (error estimation on $\hat{e}$). In Appendix A we prove the following feature of the transformation matrix $B = (b_{ij})_{i,j=1}^d$ from (4.1): If an element e fulfills the maximal angle condition and the coordinate system condition, then one can choose a reference element $\hat{e}$ such that

$$\left.\begin{aligned} |b_{jk}| &\leq C \min\{h_{j,e}, h_{k,e}\}, \quad j,k = 1,\ldots,d, \\ \left|b_{jk}^{(-1)}\right| &\leq C \min\{h_{j,e}^{-1}, h_{k,e}^{-1}\}, \quad j,k = 1,\ldots,d, \end{aligned}\right\} \tag{4.2}$$

where $b_{jk}^{(-1)}$ are the elements of B^{-1}. This property is suitable for transforming the norms from $\hat{e}$ to e, as we will see in the proof of Theorem 4.2. — After these considerations we are prepared to prove the error estimates.

Theorem 4.1 *Let $\hat{e} \subset I\!R^d$, $d = 2, 3$, be one of the reference elements introduced above, and $I^{(k)}\hat{v}$ be the Lagrangian interpolant of $\hat{v} \in W^{k+1,p}(\hat{e})$ with polynomials of order k. Then for any multi-index γ with $|\gamma| \leq k$ the estimate*

$$\|D^\gamma(\hat{v} - I^{(k)}\hat{v}); L^p(\hat{e})\| \leq C|D^\gamma \hat{v}; W^{k+1-|\gamma|,p}(\hat{e})| \tag{4.3}$$

holds if and only if

$$d = 2 \quad \textit{or} \quad \gamma \notin \{(k,0,\ldots,0),\ldots,(0,\ldots,0,k)\} \quad \textit{or} \quad p > 2. \tag{4.4}$$

Note that D^γ is always related to the coordinate system under consideration: $(x_1, \ldots, x_d)$, $(y_1, \ldots, y_d)$ or $(x_{1,e}, \ldots, x_{d,e})$, for example

$$D^\gamma v \equiv \frac{\partial^{|\gamma|} v}{\partial^{\gamma_1} x_1 \cdots \partial^{\gamma_1} x_d} \quad \text{and} \quad D^\gamma \hat{v} \equiv \frac{\partial^{|\gamma|} \hat{v}}{\partial^{\gamma_1} y_1 \cdots \partial^{\gamma_1} y_d},$$

where $v(x) = v(F(y)) = \hat{v}(x)$. Because this is always obvious, we omit a further index.
Proof The proof is a slight extension of Theorem 1 in [1], where $|\gamma| = 1$ is assumed. We use Lemma 3 of that paper with $P = \mathcal{P}_k$, $Q = \mathcal{P}_{k-|\gamma|}$, that means, it remains to find linear functionals $f_i \in (W^{k+1-|\gamma|,p}(\hat{e}))'$, $i = 1, \ldots, J$, $J = \dim \mathcal{P}_{k-|\gamma|} = \binom{k-|\gamma|+d}{d}$, with the properties

$$f_i(D^\gamma I^{(k)}\hat{v}) = f_i(D^\gamma \hat{v}), \quad i = 1,\ldots,J, \quad \textit{for all } \hat{v} \in W^{k+1,p}(\hat{e}), \tag{4.5}$$

$$\textit{if all } f_i,\ i = 1,\ldots,J, \textit{ vanish on some } q \in \mathcal{P}_{k-|\gamma|}, \textit{ then } q = 0. \tag{4.6}$$

We will illustrate this choice in four typical examples, all other cases are then canonical. In all cases one can prove (4.5) owing to $\hat{v}(y) = I^{(k)}\hat{v}(y)$ in the nodal points. For the illustration we choose the reference tetrahedron $\hat{e}$ with the vertices $(0,0,0), (1,0,0), (0,1,0)$, and $(1,0,1)$, and $k = 3$, see Figure 4.1. A cubic element is chosen because all four cases can be explained only for $k \geq 3$.

(i) For $\gamma = (2,0,0)$ we have $J = \dim \mathcal{P}_1 = 4$ and we choose

$$f_1(w) = \int_0^{\frac{1}{3}} \int_\xi^{\frac{1}{3}+\xi} w(y_1,0,0)\, dy_1 d\xi, \quad f_2(w) = \int_{\frac{1}{3}}^{\frac{2}{3}} \int_\xi^{\frac{1}{3}+\xi} w(y_1,0,0)\, dy_1 d\xi,$$

$$f_3(w) = \int_0^{\frac{1}{3}} \int_\xi^{\frac{1}{3}+\xi} w(y_1,\tfrac{1}{3},0)\, dy_1 d\xi, \quad f_4(w) = \int_{\frac{1}{3}}^{\frac{2}{3}} \int_\xi^{\frac{1}{3}+\xi} w(y_1,0,\tfrac{1}{3})\, dy_1 d\xi.$$

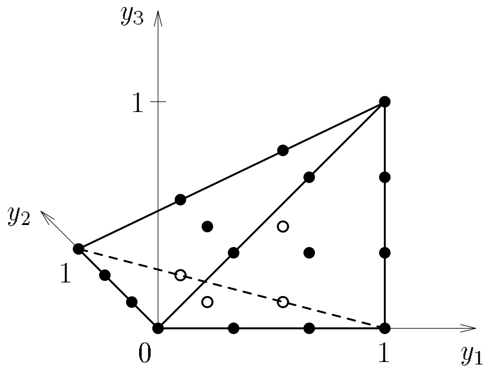

Figure 4.1: Nodes for a cubic tetrahedral element.

For $q = a_0 + a_1 y_1 + a_2 y_2 + a_3 y_3$ the functionals have the values

$$\begin{aligned} f_1(q) &= \tfrac{1}{27}(3a_0 + a_1), & f_2(q) &= \tfrac{1}{27}(3a_0 + 2a_1), \\ f_3(q) &= \tfrac{1}{27}(3a_0 + a_1 + a_2), & f_4(q) &= \tfrac{1}{27}(3a_0 + 2a_1 + a_3), \end{aligned}$$

which obviously vanish only for $a_0 = a_1 = a_2 = a_3 = 0$. Due to trace theorems we have

$$|f_i(w)| \le C\|w; L^1(\text{line})\| \le C\|w; W^{1,1}(\text{face})\| \le C\|w; W^{2,1}(\hat{e})\| \le C\|w; W^{2,p}(\hat{e})\|$$

for any $p \ge 1$, and all desired properties are proved.

(ii) For $\gamma = (1,1,0)$ we choose

$$\begin{aligned} f_1(w) &= \int_0^{\frac13}\int_0^{\frac13} w(y_1,y_2,0)\,dy_2dy_1, & f_2(w) &= \int_{\frac13}^{\frac23}\int_0^{\frac13} w(y_1,y_2,0)\,dy_2dy_1, \\ f_3(w) &= \int_0^{\frac13}\int_{\frac13}^{\frac23} w(y_1,y_2,0)\,dy_2dy_1, & f_4(w) &= \int_{\frac13}^{\frac23}\int_0^{\frac13} w(y_1,y_2,\tfrac13)\,dy_2dy_1, \end{aligned}$$

and proceed as above.

(iii) For $\gamma = (3,0,0)$ we have $J = 1$ and choose

$$f(w) = \int_0^{\frac13}\int_\xi^{\frac13+\xi}\int_\eta^{\frac13+\eta} w(y_1,0,0)\,dy_1d\eta d\xi.$$

The main difference to (i) is that this functional is bounded in $W^{1,p}(\hat{e})$ only for $p > 2$. The counterexample for $p \le 2$ in [1, page 283] extends in an obvious way to our case: For $v_\varepsilon(y) = (1 - \min\{1;\ \varepsilon \ln|\ln(r/e)|\})\,y_1^3$, $r = (y_2^2 + y_3^2)^{1/2}$, there holds

$$v_\varepsilon(j\cdot\tfrac13, 0, 0) = 0 \quad (j = 0,\dots,3), \qquad I^{(k)}v_\varepsilon(y_1,0,0) = 0, \qquad \frac{\partial^3 I^{(k)}v_\varepsilon}{\partial y_1^3} = 0,$$

$$\frac{\partial^3 v_\varepsilon}{\partial y_1^3} = 1 - \min\{1;\ \varepsilon\ \ln|\ln(r/e)|) \xrightarrow{\varepsilon\to0} 1 \quad \text{pointwise in } \hat{e}.$$

That means

$$\int_{\hat{e}} \left|\frac{\partial^3}{\partial y_1^3}(v_\varepsilon - I^{(k)}v_\varepsilon)\right|^p dy \xrightarrow{\varepsilon\to0} \operatorname{meas}_3(\hat{e}) = \frac16$$

but

$$\left|\frac{\partial^3 v}{\partial y_1^3}; W^{1,p}(\hat{e})\right|^p \le C\varepsilon \underbrace{\int_0^1 r^{-p+1}|\ln(r/e)|^{-p}dr}_{\text{bounded for } p\le2} \xrightarrow{\varepsilon\to0} 0.$$

(iv) For $\gamma = (2,1,0)$ we choose

$$f(w) = \int_0^{\frac{1}{3}} \int_{\xi}^{\frac{1}{3}+\xi} \int_0^{\frac{1}{3}} w(y_1, y_2, 0)\, dy_2 dy_1 d\xi$$

and find that this functional is bounded in $W^{1,p}(\hat{e})$ for all $p \geq 1$. $\square$

We consider now a general element $e \subset I\!R^d$, $d = 2, 3$, in the discretization independent coordinate system and transform the estimate (4.3). In order to indicate that the interpolation properties depend on the mesh, we index now the interpolation operator with an h.

Theorem 4.2 *Assume that the element e fulfills the maximal angle condition and the coordinate system condition. Then for the difference between a function $v \in W^{k+1,p}(e)$ and its Lagrangian interpolant $I_h^{(k)} v \in \mathcal{P}_k(e)$ the estimate*

$$\|D^\gamma (v - I_h^{(k)} v); L^p(e)\|^p \leq C \sum_{|\alpha| = k+1-|\gamma|} \sum_{|\beta| = |\gamma|} h_e^{\alpha p} \|D^{\alpha+\beta} v; L^p(e)\|^p \tag{4.7}$$

holds if $d = 2$ or $|\gamma| < k$ or $p > 2$.

Proof From (4.2) we obtain the relations

$$\begin{aligned}
\left|\frac{\partial v}{\partial x_{k,e}}\right| &= \left|\sum_{j=1}^d \frac{\partial v}{\partial y_j} \frac{\partial y_j}{\partial x_{k,e}}\right| \leq \sum_{j=1}^d \left|b_{jk}^{(-1)}\right| \left|\frac{\partial \hat{v}}{\partial y_j}\right| \leq C \sum_{j=1}^d \min\{h_{j,e}^{-1};\ h_{k,e}^{-1}\} \left|\frac{\partial \hat{v}}{\partial y_j}\right|, \\
\left|\frac{\partial \hat{v}}{\partial y_k}\right| &\leq C \sum_{j=1}^d \min\{h_{j,e}^{-1};\ h_{k,e}^{-1}\} \left|\frac{\partial v}{\partial x_{j,e}}\right|,
\end{aligned}$$

and conclude (in multi-index notation)

$$|D^\gamma v| \leq C \sum_{|\beta| = |\gamma|} h_e^{-\beta} |D^\beta \hat{v}|, \quad |D^\beta \hat{v}| \leq C h_e^\beta \sum_{|t| = |\beta|} |D^t v|, \quad |D^\alpha \hat{v}| \leq C \sum_{|s| = |\alpha|} h_e^s |D^s v|.$$

These estimates and Theorem 4.1 imply

$$\begin{aligned}
\|D^\gamma (v - I_h^{(k)} v); L^p(e)\|^p &\leq C \operatorname{meas}(e) \sum_{|\beta| = |\gamma|} h_e^{-\beta p} \|D^\beta (\hat{v} - I^{(k)} \hat{v}); L^p(\hat{e})\|^p \\
&\leq C \operatorname{meas}(e) \sum_{|\alpha| = k+1-|\gamma|} \sum_{|\beta| = |\gamma|} h_e^{-\beta p} \|D^{\alpha+\beta} \hat{v}; L^p(\hat{e})\|^p \\
&\leq C \sum_{|\alpha| = k+1-|\gamma|} \sum_{|\beta| = |\gamma|} h_e^{-\beta p} \sum_{|t| = |\beta|} \sum_{|s| = |\alpha|} h_e^{\beta p} h_e^{sp} \|D^{s+t} v; L^p(e)\|^p \\
&= C \sum_{|t| = |\gamma|} \sum_{|s| = k+1-|\gamma|} h_e^{sp} \|D^{s+t} v; L^p(e)\|^p,
\end{aligned}$$

and the theorem is proved. $\square$

For the case $d = 3$, $|\gamma| = k$, we can prove a weaker result for all $p \geq 1$.

Theorem 4.3 *Assume that the element e fulfills the maximal angle condition and the coordinate system condition. Then for $v \in W^{k+2,p}(e)$ the estimate*

$$\|D^\gamma (v - I_h^{(k)} v); L^p(e)\|^p \leq C \sum_{k+1-|\gamma| \leq |\alpha| \leq k+2-|\gamma|} \sum_{|\beta| = |\gamma|} h_e^{\alpha p} \|D^{\alpha+\beta} v; L^p(e)\|^p \tag{4.8}$$

holds for $d = 2, 3$, $p \geq 1$, $0 \leq |\gamma| \leq k+1$.

Proof It is sufficient to treat the cases which are not covered by the previous theorem: $d = 3$ and $|\gamma| = k$. ($|\gamma| > k$ yields the trivial case $I_h^{(k)} v = 0$.) Consider a linear functional $f \in (W^{2,p}(\hat{e}))'$ with $f(1) \neq 0$. Then

$$\left(|f(\hat{v})|^p + |\hat{v}; W^{1,p}(\hat{e})|^p + |\hat{v}; W^{2,p}(\hat{e})|^p\right)^{1/p}$$

is a norm, equivalent to $\|\hat{v}; W^{2,p}(\hat{e})\|$, see for example [14, §4.5]. Consequently,

$$\|\hat{v}; L^p(\hat{e})\|^p \leq C \left(|f(\hat{v})|^p + \sum_{1\leq|\alpha|\leq 2} \|D^\alpha \hat{v}; L^p(\hat{e})\|^p \right).$$

We proceed now as in the proof of Theorem 4.1. Because of the weaker assumption $f \in (W^{2,p}(\hat{e}))'$ instead of $f \in (W^{1,p}(\hat{e}))'$ there, we can use here the same functional f, but without the restriction $p > 2$, to get

$$\|D^\gamma(\hat{v} - I^{(k)}\hat{v}); L^p(\hat{e})\| \leq C \sum_{1\leq|\alpha|\leq 2} \|D^{\alpha+\gamma}\hat{v}; L^p(\hat{e})\|.$$

The transformation from $\hat{e}$ to e is carried out as in the proof of Theorem 4.2. □

Corollary 4.4 *Assume that the element e fulfills the maximal angle condition and the coordinate system condition. Then for $v \in W^{k+1,p}(e)$, $I_h^{(k)} v \in \mathcal{P}_k(e)$ and $m = 0, \ldots, k$, the estimate*

$$|v - I_h^{(k)} v; W^{m,p}(e)|^p \leq C \sum_{|\alpha|=k+1-m} h_e^{\alpha p} |D^\alpha v; W^{m,p}(e)|^p \tag{4.9}$$

holds, if $d = 2$ or $m < k$ or $p > 2$. If $v \in W^{k+2,p}(e)$ there holds

$$|v - I_h^{(k)} v; W^{m,p}(e)|^p \leq C \sum_{k+1-m\leq|\alpha|\leq k+2-m} h_e^{\alpha p} |D^\alpha v; W^{m,p}(e)|^p \tag{4.10}$$

for $d = 2, 3$, $m = 0, \ldots, k$, and any $p \geq 1$.

Corollary 4.5 *Assume that the element e fulfills the maximal angle condition. Then for $v \in W^{k+1,p}(e)$, $I_h^{(k)} v \in \mathcal{P}_k(e)$ and $m = 0, \ldots, k$, the estimate*

$$|v - I_h^{(k)} v; W^{m,p}(e)| \leq C h_{1,e}^{k+1-m} |v; W^{k+1,p}(e)| \tag{4.11}$$

holds, if $d = 2$ or $m < k$ or $p > 2$. If $v \in W^{k+2,p}(e)$ there holds

$$|v - I_h^{(k)} v; W^{m,p}(e)| \leq C \sum_{\ell=k+1}^{k+2} h_{1,e}^{\ell-m} |v; W^{\ell,p}(e)| \tag{4.12}$$

for $d = 2, 3$, $m = 0, \ldots, k$, and any $p \geq 1$.

Proof If we assumed the coordinate system condition the assertion follows immediately from Corollary 4.4. Because the seminorms remain equivalent during a rotation of the coordinate system, the coordinate system condition can be omitted. □

We remark that partial cases of this Corollary were proved in [4, 9, 11, 12, 19] without knowing the anisotropic estimates.

If v has the property $v \in W^{r+1,p}(e)$ with $r > k$ (or $r > k + 1$) then the estimates (4.9) and (4.11) (or (4.10) and (4.12), respectively) hold true. If $r < k$ (or $r < k + 1$) we should use $I_h^{(r)}$ for interpolation. Note that $I_h^{(r)} u \in V_h$, too. V_h is defined in (5.2).

5 The family of finite element spaces

Let $\mathcal{T}_h = \{e\}$ be an admissible triangulation of $\overline{\Omega} = \bigcup_e \overline{e}$, that means, let properties $(\mathcal{T}_h 1) \cdots (\mathcal{T}_h 5)$ of [7, Chapter 2] be fulfilled. Assume that all elements of $\mathcal{T}_h$ satisfy the maximal angle condition. Moreover, introduce the spaces V and V_h by

$$\begin{aligned} V &\equiv W_0^{1,2}(\Omega) \equiv \{v \in W^{1,2}(\Omega) : v|_{\partial\Omega} = 0\}, && (5.1)\\ V_h &\equiv \{v \in V : v|_e \in \mathcal{P}_k(e) \quad \forall e \in \mathcal{T}_h\}. && (5.2)\end{aligned}$$

The index h indicates that we are considering a family of spaces for $h \to +0$, h itself characterizes the mesh size; we can for example think of $h = \max_{e\in\mathcal{T}_h} h_{1,e}$.

Lemma 5.1 (Density of V_h in V) *Let $u \in V$ be an arbitrary function, then*

$$\lim_{h\to+0} \inf_{v_h\in V_h} \|u - v_h; W^{1,2}(\Omega)\| = 0.$$

Proof The lemma is proved in [7, Theorem 3.2.3] for isotropic elements. However, this assumption is not essential: Assume we are given an arbitrary but fixed real number $\epsilon > 0$. From a standard density argument we can determine a function $v \in V \cap W^{2,\infty}(\Omega)$ such that

$$\|u - v; W^{1,2}(\Omega)\| < \frac{\epsilon}{2}. \tag{5.3}$$

Using Corollary 4.5 we find

$$\begin{aligned} \|v - I_h^{(1)}v; W^{1,2}(\Omega)\|^2 &\leq \sum_e \mathrm{meas}_3(e)\|v - I_h^{(1)}v; W^{1,\infty}(e)\|^2 \\ &\leq C\sum_e \mathrm{meas}_3(e)\, h_{1,e}^2\|v; W^{2,\infty}(e)\|^2 \\ &\leq C\max_e h_{1,e}^2\, \mathrm{meas}_3(\Omega)\|v; W^{2,\infty}(\Omega)\|^2. \end{aligned}$$

Thus for a sufficiently small mesh size we obtain

$$\|v - v_h; W^{1,2}(\Omega)\| < \frac{\epsilon}{2}. \tag{5.4}$$

Using the triangle inequality, the assertion is proved via (5.3) and (5.4). □

6 Application to convection-diffusion problems

In this section we want to review part of the investigation of the Galerkin/Least-squares scheme which is done in [2] using the results of the previous sections. In a bounded polygonal domain $\Omega \subseteq \mathbb{R}^2$ we consider the second order elliptic boundary value problem

$$\begin{aligned} L_\varepsilon u \equiv -\varepsilon\Delta u + b\cdot\nabla u &= f \quad \text{in } \Omega && (6.1)\\ u &= 0 \quad \text{on } \partial\Omega, && (6.2)\end{aligned}$$

with the basic assumptions

(H.1) $\quad 0 < \varepsilon \leq 1$, $b \in [W^{1,\infty}(\Omega)]^d$, $f \in L^2(\Omega)$,

(H.2) $\quad \nabla\cdot b = 0$ almost everywhere in Ω.

Problem (6.1) (6.2) is a linear(ized) diffusion-convection model. In the case of large Peclet numbers $P(x) \equiv \varepsilon^{-1}\|b(x); R^d\| \gg 1$ the problem is of singularly perturbed type and the solution u may generate sharp boundary or interior layers where the solution of the limit problem with $\varepsilon = 0$ is not smooth or cannot satisfy the boundary condition (1.2). The resolution of such layers is often the main interest in applications.

On any family of meshes $\mathcal{T}_h$ satisfying elementwise the maximal angle condition we introduce the following stabilized finite element method of Galerkin/Least-squares type:

$$\textit{Find } U_h \in V_h, \textit{ such that } B_{SG}(U_h, v_h) = L_{SG}(v_h) \quad \forall v_h \in V_h. \tag{6.3}$$

with

$$B_{SG}(u,v) \equiv \varepsilon(\nabla u, \nabla v)_\Omega + \tfrac{1}{2}\{(b\cdot\nabla u, v)_\Omega - (b\cdot\nabla v, u)_\Omega\} + \sum_e \delta_e\,(L_\varepsilon u, L_\varepsilon v)_e, \tag{6.4}$$

$$L_{SG}(v) \equiv (f,v)_\Omega + \sum_e \delta_e\,(f, L_\varepsilon v)_e, \tag{6.5}$$

and a set $\{\delta_e\}$ of non-negative numerical diffusion parameters to be determined below. Here, $(.\,,.)_G$ denotes the inner product in $L^2(G)$, $G \subseteq \Omega$, and V_h is introduced in Section 5. Note that the standard Galerkin method is received for $\delta_e = 0$ for all e, but its solution may suffer from non-physical oscillations unless the mesh Peclet numbers $P_e \equiv \varepsilon^{-1}h_e\|b; [L^\infty(e)]^2\|$ are sufficiently small. — We introduce now an energy type norm according to

$$|||\, v \,|||^2_{\varepsilon,\delta} \equiv B_{SG}(v,v) = \varepsilon\|\nabla v; L^2(\Omega)\|^2 + \sum_e \delta_e\,\|L_\varepsilon v; L^2(e)\|^2.$$

For the solution U_h of (6.3) the following lemmata were proven.

Lemma 6.1 (Uniqueness and stability) *With $\delta \equiv \max_e \delta_e$ there holds for the solution $U_h \in V_h$ and the residual $L_\varepsilon U_h - f$ the estimate*

$$|||\, U_h \,|||^2_{\varepsilon,\delta} + \sum_e \delta_e\,\|L_\varepsilon U_h - f; L^2(e)\|^2 \le D^2 \equiv C(\varepsilon^{-1} + \delta)\|f; L^2(\Omega)\|^2. \tag{6.6}$$

Lemma 6.2 (Strong convergence) *Assume that (H.1), (H.2) and the technical condition $\lim\limits_{h\to+0}\max\limits_e\{\delta_e(\varepsilon C_s^2 h_{d,e}^{-2} + B_e^2\varepsilon^{-1} + C_e)\} = 0$ on the parameter set $\{\delta_e\}$ are valid. Then the solution $U_h \in V_h$ converges strongly in V to the weak solution $u \in V$ according to*

$$\lim_{h\to+0} |||\, u - U_h \,|||_{\varepsilon,0} = 0. \tag{6.7}$$

Lemma 5.1 was used in the proof. — In the case of smooth solutions as stated by

(H.3) $\quad u \in V \cap W^{r+1,2}(\Omega)$ for some $r \in I\!N$, $r \ge 1$,

the following error estimates were proved using the results of Sections 3 and 4.

Theorem 6.3 *Let (H.1), (H.2), (H.3), as well as the maximal angle condition and the coordinate system condition be satisfied. Under the assumption $\delta_e \le C_s^{-2}\varepsilon^{-1}h_{d,e}^2$ the approximation error can be estimated by*

$$|||\, u - U_h \,|||^2_{\varepsilon,\delta} \le \sum_e I_e(u), \tag{6.8}$$

$$I_e(u) \le C \sum_{|\alpha|=r-1}\sum_{|\beta|=1}\sum_{|\gamma|=1} E_{e,\beta,\gamma}\, h_e^{2(\alpha+\beta)}\|D^{\alpha+\beta+\gamma}u; L^2(e)\|^2, \tag{6.9}$$

$$E_{e,\beta,\gamma} \equiv \varepsilon + \delta_e(\varepsilon^2 h_e^{-2\beta} + B_e^2) + h_e^{2\gamma}\min\{\varepsilon^{-1}B_e^2;\ 2\delta_e^{-1}\}, \tag{6.10}$$

provided that $u \in W^{r+1,2}(\Omega)$.

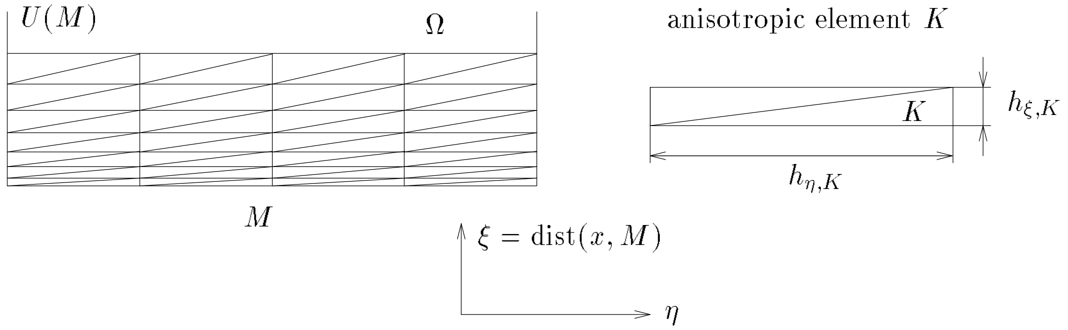

Figure 6.1: Anisotropic mesh in the boundary layer region

The parameter set $\{\delta_e\}$ is chosen by minimizing E_e^2 with respect to δ_e. The result is formulated in the following lemma for isotropic elements. Similar analysis an be done for elements in the layer, see [2].

Lemma 6.4 *The error term $I_e(u)$ of an isotropic element e (outside the refinement layer $\mathcal{R}_h$) with $h_e = \mathcal{O}(h_{1,e})$ is minimal for*

$$\delta_e = \frac{h_e^2}{\varepsilon\sqrt{1+P_e^2}} \quad \text{if} \quad P_e^2 \geq \tilde{P}_e^2 \equiv (1+\sqrt{5})/2 \tag{6.11}$$

(convection dominated case), and

$$\delta_e \leq \frac{h_e^2}{\varepsilon} \quad \text{if} \quad 0 \leq P_e \leq \tilde{P}_e \tag{6.12}$$

(diffusion dominated case). Hence there holds

$$I_e(u) \leq C\varepsilon(1+P_e)h_e^{2r}|u; W^{r+1,2}(e)|^2, \tag{6.13}$$

$1 \leq r \leq k$, $P_e \equiv B_e h_e \varepsilon^{-1}$.

The idea is now to construct a fixed mesh with anisotropic refinement in the layer regions, to use an isotropic mesh away from the layers which could be (isotropically) refined via standard adaptive methods, and to choose $h_{2,e}$ in the boundary layers in such a way that the error term $I_e(u)$ is equidistributed on $\mathcal{T}_h$. Hereby, the first task is to detect the location of the manifolds where the boundary and interior layers emanate. This can be accomplished based on a priori knowledge or a posteriori in an adaptive method, see for example [21].

For simplicity we assume that a layer of thickness $\mathcal{O}(\varepsilon^\kappa \ln \frac{1}{\varepsilon})$ is located at some straight line $M \subset \overline{\Omega}$. We introduce local coordinates (ξ, η) with $\xi = 0$ at M. As a starting point, we generate an orthogonal mesh via lines $\xi = \xi_i$, $\eta = \eta_j$ with real numbers ξ_i, η_j ($i = 0, \ldots, i_0$, $j = 0, \ldots, j_0$) and particularly $\xi_0 = 0$, $\xi_{i_0} = d(\varepsilon) \equiv \varepsilon^\kappa \ln \frac{1}{\varepsilon}$, see Figure 6.1. We assume that for a layer rectangle $K = [\xi_i, \xi_{i+1}] \times [\eta_i, \eta_{i+1}]$ the relation $h_{\xi,K} \equiv \xi_{i+1} - \xi_i \ll h_K \equiv h_{\eta,K} \equiv \eta_{j+1} - \eta_j$ holds close to M. The exceptions are geometric singularities (corners) of $M \cap \partial\Omega$ where possibly different layers intersect. Note that our approach guarantees a stronger refinement there. The rectangles K are split into 2 triangles which satisfy the maximal angle condition and the coordinate system condition with respect to the fitted coordinate system. The mesh outside the (fixed) layer regions should be of isotropic type. In this way the assumptions of Theorem 6.3 are satisfied.

There are different possibilities of the choice of $h_{\xi,K}$ and $h_{\eta,K}$. We propose $h_{\eta,K} = \mathcal{O}(h)$ with a global mesh parameter h and $h_{\xi,K} = \varepsilon^\kappa h$ if $\mathrm{dist}(e, M) \leq C_1 \varepsilon^\kappa \ln \frac{1}{\varepsilon}$. Then we double $h_{\xi,K}$ in ξ-direction (perpendicularly to M) until $\xi = C_2 h^\kappa \ln \frac{1}{h}$ and choose $h_{\xi,K} = \mathcal{O}(h)$ if $\xi \geq C_2 h^\kappa \ln \frac{1}{h}$. In [2] we present a more detailed analysis for boundary layers of outflow type ($\kappa = 1$) and characteristic layers ($\kappa = 0.5$) and derive global error estimates with respect to

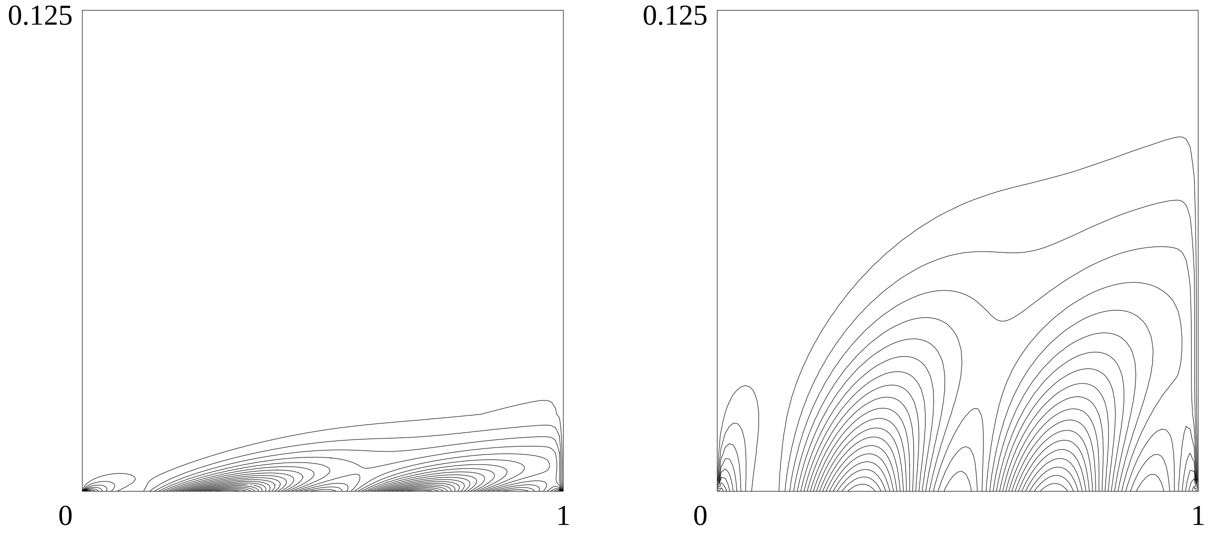

Figure 6.2: Isoline plots for $\varepsilon = 10^{-4}$, $\alpha = 0$ and $\alpha = 1$

the norm $|||\ .\ |||_{\varepsilon,\delta}$ which are uniformely valid for $\varepsilon \to +0$. The critical point is an assumption on Sobolev norm estimates of u in the neighbourhood of M which are hard to prove.

The following illustrative example is concerned with characteristic layers. Let $\Omega = (0,1)^2$ and

$$\begin{aligned} -\varepsilon\Delta u + x_2^\alpha \frac{\partial u}{\partial x_1} &= 0 && \text{in } \Omega, \\ u &= \sin(5\pi x_1) && \text{on } \{x \in \partial\Omega : x_2 = 0\}, \\ u &= 1 && \text{elsewhere.} \end{aligned}$$

A characteristic layer appears at $M = (0,1) \times \{0\}$, it has the thickness $\mathcal{O}(\varepsilon^\kappa \ln \frac{1}{\varepsilon})$ with $\kappa = (2\alpha+2)^{-1}$. The resolution of the layer is accomplished via an anisotropic boundary layer mesh with $h_\eta = h = 1/128$ and $h_\xi = \varepsilon^\kappa h$ if $0 \le \xi \equiv x_2 \le \varepsilon^\kappa \ln \frac{1}{\varepsilon}$. An isoline plot is shown in Figure 6.2 for $\varepsilon = 10^{-4}$, $\alpha = 0$ and $\alpha = 1$. The layer at $x_2 = 0$ is obviously enlarged under the no-slip condition for the field $b = \begin{pmatrix} x_2 \\ 0 \end{pmatrix}$ compared with the slip condition $b = \begin{pmatrix} 1 \\ 0 \end{pmatrix}$ for $\alpha = 0$. — We found a resolution of the boundary layer with about 48 000 elements of the same quality as with an isotropic uniform mesh with about 2 million elements.

7 Discussion of the maximal angle and the coordinate system conditions

In this last section we discuss the necessity of the conditions.

Lemma 7.1 *If the maximal angle condition is not fulfilled, then Theorem 4.2 is not valid.*

Proof In the two-dimensional case, we consider the triangle e with the vertices $(0,0)$, $(h_1,0)$, $(\frac{1}{2}h_1, h_2)$, and $v = x_1^2$. One can directly calculate that

$$\frac{\left\| \frac{\partial}{\partial x_2}(v - I_h v); L^2(e) \right\|^2}{\sum\limits_{|\alpha|=1} \sum\limits_{|\beta|=1} h_e^{2\alpha} \|D^{\alpha+\beta} v; L^2(e)\|^2} \sim \frac{h_1^5 h_2^{-1}}{h_1^3 h_2} = \left(\frac{h_1}{h_2}\right)^2 \sim \cot^2\gamma_e \to \infty.$$

From this we get immediately the necessity of the maximal angle condition for the angles of the faces of a tetrahedron. At last, consider an example where this condition is satisfied, but not the condition to the angles at the edges: For the tetrahedron with the vertices $(0,0,0)$, $(h,0,0)$, $(0,h,0)$, and $(\frac{1}{3}h, \frac{1}{3}h, h^\alpha)$ $(\alpha > 1)$ and for $v = x_1^2$ we find

$$\begin{aligned}
\sum_{|\alpha|=1} h^{\alpha p} |D^\alpha v; W^{1,p}(e)|^p &= (2h)^p \mathrm{meas}_3(e), \\
I_h v &= h x_1 - \tfrac{2}{9} h^{2-\alpha} x_3, \\
\left\| \frac{\partial}{\partial x_3}(v - I_h v); L^p(e) \right\|^p &= \left(\tfrac{2}{9} h^{2-\alpha}\right)^p \mathrm{meas}_3(e),
\end{aligned}$$

and, consequently,

$$\frac{\left\| \frac{\partial}{\partial x_3}(v - I_h v); L^p(e) \right\|^p}{\sum\limits_{|\alpha|=1} h^{\alpha p} |D^\alpha v; W^{1,p}(e)|^p} = \left(\tfrac{1}{9} h^{1-\alpha}\right)^p \xrightarrow[h\to 0]{\alpha>1} \infty.$$

We remark that the case $p = \infty$ was already considered in [12, Examples 8, 9]. □

As seen in the proof of Lemma 7.1, there are elements which satisfy the maximal angle condition related to the triangular faces but not for the angles at the edge. Also the converse is true, see [12, Example 9]. That means, both conditions are independent.

At this point we want to remark that an uncontrolable growth of the interpolation error for degenerate elements gives no information about the approximation error of the corresponding finite element method. In the literature we can find two examples where triangles with large angles are considered and the interpolation error in the $W^{1,2}$-norm grows to infinity. But while in [4] the finite element error grows to infinity as well, there is an example in [1] where a modified interpolate and thus the finite element solution converge.

The following numerical example underlines the necessity of the coordinate system condition. Consider again the unit square and

$$\begin{aligned}
-\varepsilon \Delta u + \begin{pmatrix} 1 \\ 0.5 \end{pmatrix} \cdot \nabla u &= 0 \quad \text{in } \Omega, \\
u &= 1 \quad \text{on } \{x \in \partial\Omega : x_1 = 0,\ 0.25 \le x_2 \le 1\}, \\
u &= 0 \quad \text{elsewhere on } \partial\Omega.
\end{aligned}$$

An interior layer emanates from the discontinuity at $(0, 0.25)$ along the manifold $M_1 = \{x \in \Omega : x_2 = 0.5x_1 + 0.25\}$ and intersects at $(1, 0.75)$ with a boundary layer along $M_2 = [(0,1) \times \{1\}] \cup [\{1\} \times (0.75, 1)]$. An anisotropic mesh is constructed in the neighbourhood of M_1 and M_2 similarly to the proposal in Section 6. The maximal aspect ratio is about $h_{\eta,K}/h_{\xi,K} = 240$. The layers are well resolved for $\varepsilon = 10^{-4}$ if the coordinate system condition is satisfied with respect to an orthogonal coordinate system with the η-axis at M_1, compare Figure 7.1(a). On the other hand, wiggles occur at M_1 if the angle between M_1 and the η-axis is 2°, see Figure 7.1(b).

A Properties of the transformation to a reference element

In this Appendix we will show that the geometrical description of finite elements by the *maximal angle condition* and the *coordinate system condition* is sufficient for the more abstract condition (4.2) on the elements of the transformation matrix B in (4.1). For this we will split the transformation (4.1) into two parts:

$$x = B_1 x_e + \tilde{b}, \qquad x_e = B_2 y + b_2, \tag{A.1}$$

with $B = B_1 B_2$ and $\tilde{b} = b - B_1 b_2$. The notation was introduced in Sections 2 and 4.

We start with the two-dimensional case, consider the reference element $\hat{e}$ with the nodes $(0,0)$, $(1,0)$, and $(0,1)$, and remark that the assertion is implicitely contained in the proof of Theorem 2 of [1].

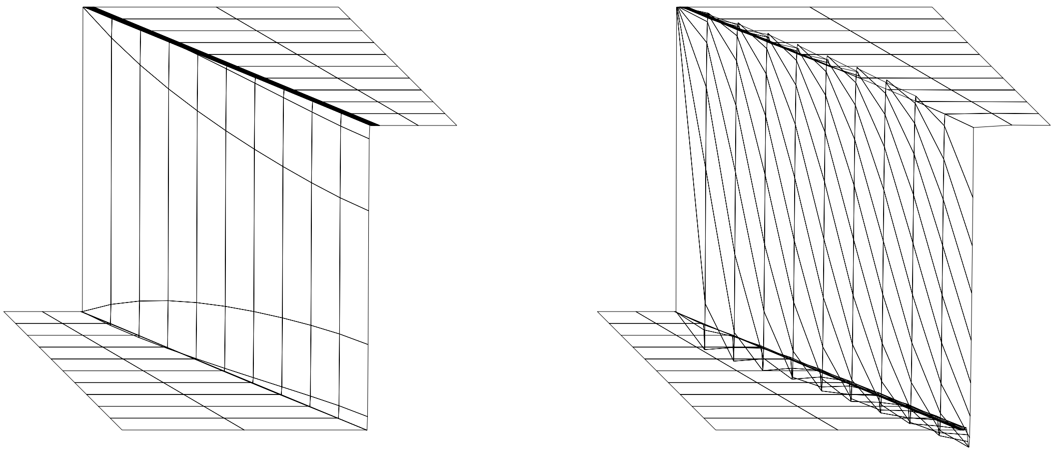

(a) (b)

Figure 7.1: Dependence of the resolution of an internal layer on the satisfaction of the coordinate system condition

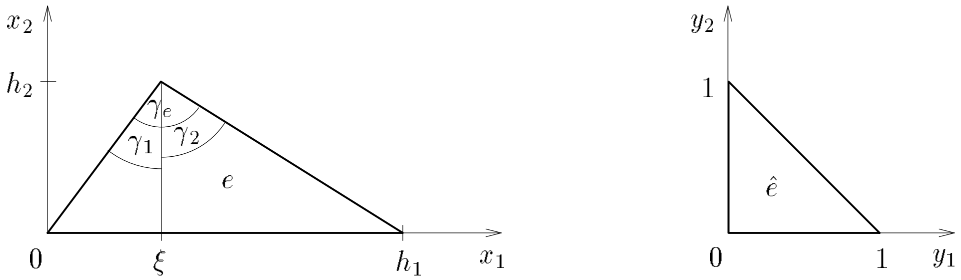

Figure A.1: Notation and illustration of the two-dimensional case.

Lemma A.1 *Assume that an element $e \subset I\!R^d$, $d = 2$, satisfies the maximal angle condition (see Subsection 4.1). Then the elements of matrix $B_2 = \left(b_{jk}^{(2)}\right)_{j,k=1}^{d}$ fulfill the relations*

$$\left.\begin{array}{rcccll} 0 & < & C_1 h_{j,e} \le & |b_{jj}^{(2)}| & \le C_2 h_{j,e} & \text{for } j = 1, \ldots, d, \\ & & & |b_{jk}^{(2)}| & \le C \min\{h_{j,e}, h_{k,e}\} & \text{for } j,k = 1, \ldots, d, \end{array}\right\} \tag{A.2}$$

Proof For simplicity we omit in the proof the upper index of the elements of the matrix (b_{jk} instead of $b_{jk}^{(2)}$) and the second index e (h_i instead of $h_{i,e}$, x_i instead of $x_{i,e}$). Introduce the notation as illustrated in Figure A.1 and consider first the case $\xi < \frac{1}{2}h_1$. By

$$\cot\gamma_e = \frac{\cot\gamma_1 \cot\gamma_2 - 1}{\cot\gamma_1 + \cot\gamma_2} = \frac{h_2}{h_1} - \frac{\xi(h_1 - \xi)}{h_1 h_2}$$

we get using $\gamma_e < \gamma_*$ and Taylor's formula for $\sqrt{1+2x}$

$$\xi = \frac{h_1}{2}\left\{1 - \sqrt{1 + 2\left(2\frac{h_2}{h_1}\cot\gamma_e - 2\left(\frac{h_2}{h_1}\right)^2\right)}\right\} = -h_2 \cot\gamma_e + h_1\, o\left(\frac{h_2}{h_1}\right) \le C h_2.$$

With

$$B_2 = \begin{pmatrix} h_1 & \xi \\ 0 & h_2 \end{pmatrix}$$

the relations (A.2) can be concluded.

The case $\xi > \frac{1}{2}h_1$ is traced back via a reflection at $x_1 = \frac{1}{2}h_1$ to the previous case. Note that reflections at coordinate planes and translations do not influence condition (A.2). $\square$

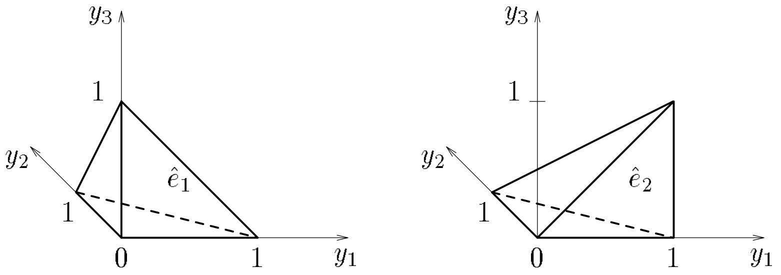

Figure A.2: Reference elements in the three-dimensional case.

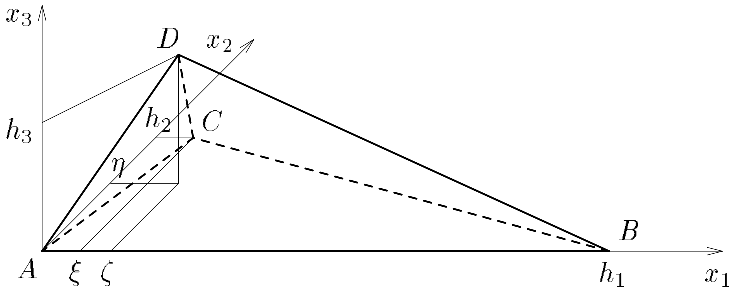

Figure A.3: Notation and illustration of Case 1 in three dimensions.

In the three-dimensional case, it is necessary to consider two reference elements $\hat{e}_1$ and $\hat{e}_2$, as given in Figure A.2. Note that anisotropic elements can have three or four edges with length of order h_1. They are mapped to $\hat{e}_1$ and $\hat{e}_2$, respectively.

Lemma A.2 *Assume that an element $e \subset I\!\!R^3$ satisfies the maximal angle condition (see Subsection 4.1). Then one can choose $\hat{e}_1$ or $\hat{e}_2$ as the reference element such that the elements of matrix $B_2 = \left(b_{jk}^{(2)}\right)_{j,k=1}^3$ fulfill (A.2).*

Proof We consider three main cases, all other cases are equivalent to one of them by reflection at coordinate planes and translation.

Case 1. Consider the situation as given in Figure A.3 with

$$0 < \xi < \frac{h_1}{2}, \quad -h_2 < \eta < \frac{h_2}{2}, \quad 0 < \zeta < \frac{h_1}{2}. \tag{A.3}$$

(AB is the largest edge.) As in the two-dimensional case, we get from $\sphericalangle ACB \le \gamma_* < \pi$ that $0 < \xi < C\, h_2$. With the same technique we find

$$\begin{aligned} \cot \sphericalangle ADB &= \frac{\sqrt{h_3^2 + \eta^2}}{h_1} - \frac{\zeta(h_1 - \zeta)}{h_1 \sqrt{h_3^2 + \eta^2}}, \\ \zeta &\le C \sqrt{h_3^2 + \eta^2}. \end{aligned} \tag{A.4}$$

That means immediately

$$\zeta \le C h_2 \tag{A.5}$$

but we will improve this later. For η we have to distinguish the cases $\eta < 0$ and $\eta > 0$, and we will consider the angles at the edges AB and BD, respectively. Generally, an angle φ at some edge can be expressed as follows: Let n_1 and n_2 be the outer normals of the faces forming the edge, then

$$\cos \varphi = -\frac{n_1 \cdot n_2}{|n_1||n_2|} \quad \text{and} \quad \sin \varphi = \frac{|n_1 \times n_2|}{|n_1||n_2|}.$$

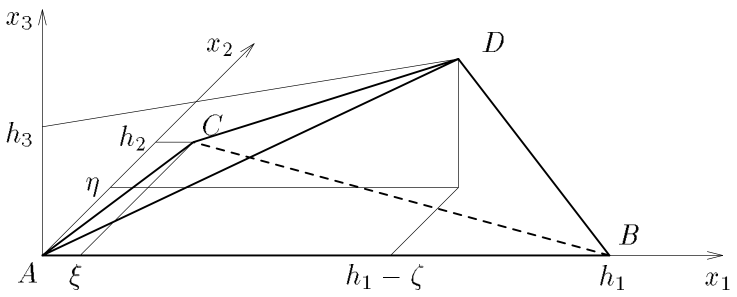

Figure A.4: Notation and illustration of Case 2 in three dimensions.

Via goniometric identities we imply for $\tan\frac{\varphi}{2}$ the expression

$$\tan\frac{\varphi}{2}=\frac{1-\cos\varphi}{1+\cos\varphi}=\frac{(1-\cos\varphi)^2}{\sin^2\varphi}=\frac{(|n_1||n_2|+n_1\cdot n_2)^2}{|n_1\times n_2|^2}$$

which is bounded if and only if $\varphi\leq\gamma_*<\pi$. Using

$$n_{ABC}=\begin{pmatrix}0\\0\\-1\end{pmatrix},\quad n_{ABD}=\begin{pmatrix}0\\-h_3\\\eta\end{pmatrix},\quad n_{BCD}=\begin{pmatrix}h_2h_3\\h_3(h_1-\xi)\\h_2(h_1-\zeta)-\eta(h_1-\xi)\end{pmatrix}$$

we get for the case $\eta<0$

$$\tan\frac{\gamma_*}{2}\geq\tan\frac{\varphi_{AB}}{2}=\frac{\left[\sqrt{\eta^2+h_3^2}-\eta\right]^2}{h_3^2}=\left(\frac{\eta}{h_3}\right)^2\left[\sqrt{1+\left(\frac{h_3}{\eta}\right)^2}+1\right]^2>4\left(\frac{\eta}{h_3}\right)^2,\qquad\text{(A.6)}$$

consequently $|\eta|<Ch_3$.

Using $\chi\equiv h_1h_2+\xi\eta-h_1\eta-h_2\zeta$ and $\sqrt{a^2+b^2}\geq\max\{|a|;|b|\}$, we conclude for the case $\eta>0$

$$\begin{aligned}\tan\frac{\gamma_*}{2}&\geq\tan\frac{\varphi_{BD}}{2}=\frac{\left[\sqrt{\eta^2+h_3^2}\sqrt{h_2^2h_3^2+h_3^2(h_1-\xi)^2+\chi^2}-h_3^2(h_1-\xi)+\eta\chi\right]^2}{\left[h_3\eta(h_1-\xi)+h_3\chi\right]^2+\left[\eta h_2h_3\right]^2+\left[h_2h_3^2\right]^2}\\&\geq\frac{\eta^2\chi^2}{h_2^2h_3^2\left[(h_1-\zeta)^2+\eta^2+h_3^2\right]}=\left(\frac{\eta}{h_3}\right)^2\frac{\left[1+\frac{\xi\eta}{h_1h_2}-\frac{\eta}{h_2}-\frac{\zeta}{h_1}\right]^2}{\left(1-\frac{\zeta}{h_1}\right)^2+\left(\frac{\eta}{h_1}\right)^2+\left(\frac{h_3}{h_1}\right)^2}.\end{aligned}$$

With (A.3), (A.5), we find

$$1+\frac{\xi\eta}{h_1h_2}-\frac{\eta}{h_2}-\frac{\zeta}{h_1}\geq C>0\quad\text{and}\quad\left(1-\frac{\zeta}{h_1}\right)^2+\left(\frac{\eta}{h_1}\right)^2+\left(\frac{h_3}{h_1}\right)^2\leq C.$$

Consequently, we get $\eta<Ch_3$, and with (A.4) $\zeta<Ch_3$. Realizing that

$$B_2=\begin{pmatrix}h_1&\xi&\zeta\\0&h_2&\eta\\0&0&h_3\end{pmatrix}$$

for the reference element $\hat{e}_1$, condition (A.2) is concluded.

Case 2: Consider the situation in Figure A.4 with (A.3) being valid again. The transformation to $\hat{e}_2$ is

$$x_e=\begin{pmatrix}h_1&\xi&-\zeta\\0&h_2&\eta\\0&0&h_3\end{pmatrix}y,$$

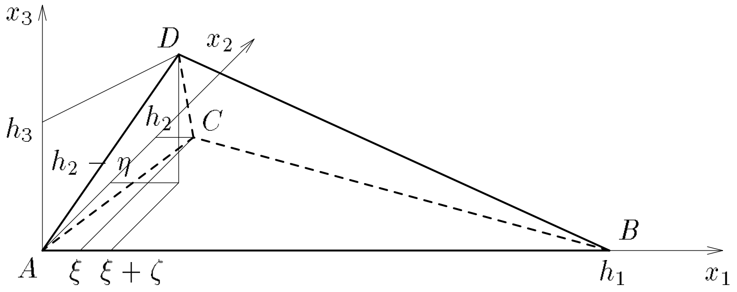

Figure A.5: Notation and illustration of Case 3 in three dimensions.

and as above one can show relation (A.2): $\sphericalangle ACB \le \gamma_* < \pi$ and $\sphericalangle ADB \le \gamma_* < \pi$ lead to

$$\xi \le Ch_2 \quad \text{and} \quad \zeta \le C\sqrt{h_3^2+\eta^2} \le Ch_2, \tag{A.7}$$

respectively. For $\eta < 0$, we get $|\eta| \le Ch_3$ from (A.6). For $\eta > 0$, we use $n_{ABD} = (0, -h_3, \eta)^T$, $n_{ADC} = (-h_2h_3, \xi h_3, \chi)^T$ with $\chi \equiv h_2(h_1-\zeta) - \xi\eta$, and find

$$\begin{aligned}
\tan\frac{\gamma_*}{2} &\ge \tan\frac{\varphi_{AD}}{2} = \frac{\left[\sqrt{\eta^2+h_3^2}\sqrt{h_2^2h_3^2+\xi^2h_3^2+\chi^2}+\xi h_3^2-\eta\chi\right]^2}{[\chi h_3+\xi\eta h_3]^2+[\eta h_2h_3]^2+[h_2h_3^2]^2} \\
&\ge \frac{\eta^2\chi^2}{h_2^2h_3^2\left[(h_1-\zeta)^2+\eta^2+h_3^2\right]} = \left(\frac{\eta}{h_3}\right)^2 \frac{h_1^2h_2^2\left[1-\frac{\zeta}{h_1}-\frac{\xi}{h_1}\frac{\eta}{h_2}\right]^2}{h_1^2h_2^2\left[\left(1-\frac{\zeta}{h_1}\right)^2+\left(\frac{\eta}{h_1}\right)^2+\left(\frac{h_3}{h_1}\right)^2\right]}.
\end{aligned}$$

With (A.3) and (A.7) we conclude that $|\eta| < Ch_3$ and $\zeta < Ch_3$.

Case 3: The situation is illustrated in Figure A.5 and we assume

$$0 \le \xi < \frac{h_1}{2}, \quad 0 \le \eta \le \frac{h_2}{2}, \quad 0 \le \xi+\zeta \le \frac{h_1}{2}. \tag{A.8}$$

The transformation to $\hat{e}_1$ is

$$x_e = \begin{pmatrix} h_1-\xi & -\xi & \zeta \\ -h_2 & -h_2 & -\eta \\ 0 & 0 & h_3 \end{pmatrix} y + \begin{pmatrix} \xi \\ h_2 \\ 0 \end{pmatrix}.$$

From $\sphericalangle ACB \le \gamma_* < \pi$ and $\sphericalangle ADB \le \gamma_* < \pi$ we get $\xi \le Ch_2$ and $\xi+\zeta \le Ch_2$. Furthermore, we consider φ_{AD}: Using $n_{ABD} = (0, -h_3, h_2-\eta)^T$, $n_{ADC} = (-h_2h_3, \xi h_3, \chi)^T$, $\chi \equiv h_2\zeta + \xi\eta$, we obtain

$$\begin{aligned}
\tan\frac{\gamma_*}{2} &\ge \tan\frac{\varphi_{AD}}{2} = \frac{\left[\sqrt{h_3^2+(h_2-\eta)^2}\sqrt{h_2^2h_3^2+\xi^2h_3^2+\chi^2}-\xi h_3^2+(h_2-\eta)\chi\right]^2}{h_2^2h_3^2\left[(\zeta+\xi)^2+(h_2-\eta)^2+h_3^2\right]} \\
&\ge \frac{(h_2-\eta)^2}{(\zeta+\xi)^2+(h_2-\eta)^2+h_3^2}\cdot\frac{\chi^2}{h_2^2h_3^2} = \frac{(\frac{1}{2}h_2)^2}{Ch_2^2}\cdot\frac{\chi^2}{h_2^2h_3^2}.
\end{aligned}$$

Consequently, it is

$$|\chi| = |h_2\zeta + \xi\eta| \le Ch_2h_3. \tag{A.9}$$

Additionally, we consider φ_{BD}: Using $n_{ABD} = (0, -h_3, h_2-\eta)^T$, $n_{BCD} = (h_2h_3, h_3(h_1-\xi), h_1\eta-\chi)^T$, χ as before, we obtain

$$\tan\frac{\gamma_*}{2} \ge \tan\frac{\varphi_{BD}}{2}$$

$$
= \frac{\left[\sqrt{h_3^2+(h_2-\eta)^2}\sqrt{h_2^2h_3^2+(h_1-\xi)^2h_3^2+(h_1\eta-\chi)^2}-(h_1-\xi)h_3^2+(h_2-\eta)(h_1\eta-\chi)\right]^2}{h_2^2h_3^2\left[(h_1-\zeta-\xi)^2+(h_2-\eta)^2+h_3^2\right]}
$$

$$
\geq \frac{(h_2-\eta)^2(h_1\eta-\chi)^2}{h_2^2h_3^2\left[(h_1-\zeta-\xi)^2+(h_2-\eta)^2+h_3^2\right]} \geq \frac{(\frac{1}{2}h_2)^2(h_1\eta-\chi)^2}{Ch_1^2h_2^2h_3^2} = \frac{1}{C}\left(\frac{\eta}{h_3}-\frac{\chi}{h_2h_3}\right)^2,
$$

that means

$$
\frac{\chi}{h_2h_3}-\sqrt{C\tan\frac{\gamma_*}{2}} \leq \frac{\eta}{h_3} \leq \frac{\chi}{h_2h_3}+\sqrt{C\tan\frac{\gamma_*}{2}},
$$

and with (A.9) $\eta \leq Ch_3$. Consequently, (A.9), $\xi \leq Ch_2$, and $\eta \leq Ch_3$ lead to $\zeta \leq Ch_3$.

Other cases: The situations $C=(\xi,h_2,0)$, $D=(\zeta,\eta,-h_3)$, and $C=(h_1-\xi,h_2,0)$, $D=(h_1-\zeta,\eta,\pm h_3)$, (A.3) being valid in each case, are equivalent to Case 1; $C=(\xi,h_2,0)$, $D=(h_1-\zeta,\eta,-h_3)$, and $C=(h_1-\xi,h_2,0)$, $D=(\zeta,\eta,\pm h_3)$, (A.3) being valid as well, are traced back to Case 2; $C=(\xi,h_2,0)$, $D=(\zeta,h_2-\eta,-h_3)$, and $C=(h_1-\xi,h_2,0)$, $D=(h_1-\zeta,h_2-\eta,\pm h_3)$, (A.8) being valid in these cases, are equivalent to Case 3. Note that there are no further cases. Particularly, a situation as $C=(\xi,h_2,0)$, $D=(h_1-\zeta,h_2-\eta,\pm h_3)$, is impossible because $\varphi_{AD}\to\pi$. □

Lemma A.3 *Assume that an element $e\subset I\!R^d$, $d=2,3$, satisfies the coordinate system condition (see Section 2). Then the elements of matrix $B_1=\left(b_{jk}^{(1)}\right)_{j,k=1}^{d}$ satisfy the relations*

$$
\left.\begin{array}{rcccll}
0 < C_1 & \leq & |b_{jj}^{(1)}| & \leq & C_2 & \text{for } j=1,\ldots,d, \\
 & & |b_{jk}^{(1)}| & \leq & Ch_{j,e}/h_{k,e} & \text{for } k=1,\ldots,j-1, \quad j=2,\ldots,d, \\
 & & |b_{jk}^{(1)}| & \leq & Ch_{k,e}/h_{j,e} & \text{for } k=j+1,\ldots,d, \quad j=1,\ldots,d.
\end{array}\right\} \qquad (A.10)
$$

Proof We give here the proof for $d=3$; in the two-dimensional case the proof is similar. B_1 is a product of three matrices B_{11}, B_{12}, B_{13}, describing rotations:

$$
B_{11}=\begin{pmatrix} 1 & 0 & 0 \\ 0 & \cos\psi_{1,e} & \sin\psi_{1,e} \\ 0 & -\sin\psi_{1,e} & \cos\psi_{1,e}\end{pmatrix}, \quad B_{12}=\begin{pmatrix} \cos\psi_{2,e} & 0 & \sin\psi_{2,e} \\ 0 & 1 & 0 \\ -\sin\psi_{2,e} & 0 & \cos\psi_{2,e}\end{pmatrix},
$$

$$
B_{13}=\begin{pmatrix} \cos\psi_{3,e} & \sin\psi_{3,e} & 0 \\ -\sin\psi_{3,e} & \cos\psi_{3,e} & 0 \\ 0 & 0 & 1\end{pmatrix}.
$$

Using (2.1) and $|\cos\psi_{i,e}|\geq C$ $(i=1,\ldots,d)$ one can compute (A.10). □

Theorem A.4 *One can choose a reference element such that the elements of the matrix $B=B_1B_2$ satisfies the relations (4.2). In two dimensions the reference element can be chosen as in Figure A.1, in three dimensions we use two reference elements, see Figure A.2.*

Proof The first relation in (4.2) is a consequence of Lemmata A.1 – A.3. The second relation can be proved via the explicit formula for the coefficients of the inverse matrix B^{-1}. □

Acknowledgement. The first author was supported by DFG (German Research Foundation), No. La 767-3/1. The calculations were done by A. Kapurkin and D. Weiß at the University of Magdeburg. All this help and support is gratefully acknowledged.

References

[1] Th. Apel and M. Dobrowolski. Anisotropic interpolation with applications to the finite element method. *Computing*, 47:277–293, 1992.

[2] Th. Apel and G. Lube. Anisotropic mesh refinement in stabilized galerkin methods. Preprint SPC95_1, TU Chemnitz-Zwickau, 1995. In preparation.

[3] Th. Apel and S. Nicaise. Elliptic problems in domains with edges: anisotropic regularity and anisotropic finite element meshes. Preprint SPC94_16, TU Chemnitz-Zwickau, 1994.

[4] I. Babuška and A.K. Aziz. On the angle condition in the finite element method. *SIAM J. Numer. Anal.*, 13(2):214–226, April 1976.

[5] J. H. Bramble and S. R. Hilbert. Estimation of linear functionals on Sobolev spaces with applications to Fourier transforms and spline interpolation. *SIAM J. Num. Anal.*, 7:112–124, 1970.

[6] J. H. Bramble and S. R. Hilbert. Bounds for a class of linear functionals with applications to Hermite interpolation. *Numerische Mathematik*, 16:362–369, 1971.

[7] P. Ciarlet. *The finite element method for elliptic problems.* North-Holland Publishing Company, Amsterdam, 1978.

[8] W. Guo and M. Stynes. Pointwise error estimates for a streamline diffusion scheme on a Shishkin mesh for a convection-diffusion problem. Submitted for publication.

[9] P. Jamet. Estimations d'erreur pour des éléments finis droits presque dégénérés. *R.A.I.R.O. Anal. Numér.*, 10(3):43–61, 1976.

[10] R. Kornhuber and R. Roitzsch. On adaptive grid refinement in the presence of internal and boundary layers. *IMPACT of Computing in Sci. and Engrg.*, 2:40–72, 1990.

[11] M. Křížek. On semiregular families of triangulations and linear interpolation. *Appl. Math.*, 36(3):223–232, 1991.

[12] M. Křížek. On the maximum angle condition for linear tetrahedral elements. *SIAM J. Num. Anal.*, 29(2):513–520, 1992.

[13] J. Lang. An adaptive finite element method for convection-diffusion problems by interpolation techniques. Technical Report TR 91–4, ZIB Berlin, 1991.

[14] S. G. Michlin. *Partielle Differentialgleichungen in der mathematischen Physik.* Akademie-Verlag, Berlin, 1978.

[15] J. Peraire, M. Vahdati, K. Morgan, and O. C. Zienkiewicz. Adaptive remeshing for compressible flow computation. *J. Comp. Phys.*, 72:449–466, 1987.

[16] T. von Petersdorff. *Randwertprobleme der Elastizitätstheorie für Polyeder – Singularitäten und Approximationen mit Randelementmethoden.* PhD thesis, TH Darmstadt, 1989.

[17] W. Rachowicz. An anisotropic h-type mesh refinement strategy. *Comput. Methods Appl. Mech. Engrg.*, 109:169–181, 1993.

[18] K. Siebert. An a posteriori error estimator for anisotropic refinement. Preprint 313, Universität Bonn, SFB 256, 1993.

[19] J. L. Synge. *The hypercircle in mathematical physics.* Cambridge University Press, Cambridge, 1957.

[20] G. Zhou and R. Rannacher. Mesh orientation and anisotropic refinement in the streamline diffusion method. Preprint 93-57, Universität Heidelberg, IWR, SFB 359, 1993.

[21] O. C. Zienkiewicz and J. Wu. Automatic directional refinement in adaptive analysis of compressible flows. *Int. J. Num. Meth. Eng.*, 37:2189–2210, 1994.

Other titles in the SPC series:

93_1 G. Haase, T. Hommel, A. Meyer and M. Pester. Bibliotheken zur Entwicklung paralleler Algorithmen. May 1993.

93_2 M. Pester and S. Rjasanow. A parallel version of the preconditioned conjugate gradient method for boundary element equations. June 1993.

93_3 G. Globisch. PARMESH – a parallel mesh generator. June 1993.

94_1 J. Weickert and T. Steidten. Efficient time step parallelization of full-multigrid techniques. January 1994.

94_2 U. Groh. Lokale Realisierung von Vektoroperationen auf Parallelrechnern. March 1994.

94_3 A. Meyer. Preconditoning the Pseudo-Laplacian for Finite Element simulation of incompressible flow. February 1994.

94_4 M. Pester. Bibliotheken zur Entwicklung paralleler Algorithmen. (aktualisierte Fassung). March 1994.

94_5 U. Groh, Chr. Israel, St. Meinel and A. Meyer. On the numerical simulation of coupled transient problems on MIMD parallel systems. April 1994.

94_6 G. Globisch. On an automatically parallel generation technique for tetrahedral meshes. April 1994.

94_7 K. Bernert. Tauextrapolation – theoretische Grundlagen, numerische Experimente und Anwendungen auf die Navier-Stokes-Gleichungen. June 1994.

94_8 G. Haase, U. Langer, A. Meyer and S. V. Nepomnyaschikh. Hierarchical extension and local multigrid methods in domain decomposition preconditoners. June 1994.

94_9 G. Kunert. On the choice of the basis transformation for the definition of DD Dirichlet preconditioners. June 1994.

94_10 M. Pester and T. Steidten. Parallel implementation of the Fourier Finite Element Method. June 1994.

94_11 M. Jung and U. Rüde. Implicit Extrapolation Methods for Multilevel Finite Element Computations: Theory and Applications. June 1994.

94_12 A. Meyer and M. Pester. Verarbeitung von Sparse-Matrizen in Kompaktspeicherform (KLZ/KZU). June 1994.

94_13 B. Heinrich and B. Weber. Singularities of the solution of axisymmetric elliptic interface problems. June 1994.

94_14 K. Gürlebeck, A. Hommel and T. Steidten. The method of lumped masses in cylindrical coordinates. July 1994.

94_15 Th. Apel and F. Milde. Realization and comparison of various mesh refinement strategies near edges. August 1994.

94_16 Th. Apel and S. Nicaise. Elliptic problems in domains with edges: anisotropic regularity and anisotropic finite element meshes. August 1994.

94_17 B. Heinrich. The Fourier-finite-element method for Poisson's equation in axisymmetric domains with edges. August 1994.

94_18 M. Pester and S. Rjasanow. A parallel preconditioned iterative realization of the panel method in 3D. September 1994.

94_19 A. Meyer. Preconditoning the Pseudo-Laplacian for Finite Element simulation of incompressible flow. October 1994.

94_20 V. Mehrmann. A step towards a unified treatment of continous and discrete time control problems. October 1994.

94_21 C. He, V. Mehrmann. Stabilization of large linear systems. October 1994.

94_22 B. Heinrich and B. Weber. The Fourier-finite-element method for three-dimensional elliptic problems with axisymmetric interfaces. November 1994.

94_23 M. Pester. On-line visualization in parallel computations. November 1994.

94_24 M. Pester. Grafik-Ausgabe vom Parallelrechner für 2D-Gebiete. November 1994.

94_25 R. Byers, C. He, V. Mehrmann. The Matrix Sign Function Method and the Computation of Invariant Subspaces. November 1994.

Some papers can be accessed via anonymous ftp from server `ftp.tu-chemnitz.de`, directory `pub/Local/mathematik/SPC`. (Note the capital L in Local!)